Journal of Alloys and Compounds 889 (2021) 161556

Contents lists available at ScienceDirect

Journal of Alloys and Compounds

journal homepage: www.elsevier.com/locate/jalcom

# Synthesis and dielectric properties in the lithium-ion conducting material $La_{0.5}Li_{0.5-x}Na_xTiO_3$

O.I. V'yunov[a,*], T.O. Plutenko[a], O.P. Fedorchuk[a], A.G. Belous[a], Ye.V. Lobko[b]

[a] V.I. Vernadsky Institute of General and Inorganic Chemistry NAS of Ukraine, Kyiv, Ukraine
[b] Charles University, Praha, Czech Republic

ARTICLE INFO

*Article history:*
Received 9 June 2021
Received in revised form 3 August 2021
Accepted 10 August 2021
Available online 12 August 2021

*Keywords:*
Perovskite
Ceramic
Grain size
Impedance spectroscopy
High dielectric constant

ABSTRACT

Ceramic samples of Na-doped lithium lanthanum titanates have been synthesized by solid-state reaction technique. Scanning electron microscopy has shown that the grain size of ceramics in $La_{0.5}Li_{0.5-x}Na_xTiO_3$ solid solutions decreases with an increase in sodium concentration. Complex impedance spectroscopy measurements demonstrate that the origin of the electrical properties in $La_{0.5}Li_{0.5-x}Na_xTiO_3$ can be attributed to equivalent circuit consist of 3 elements, when x=0–0.4 and 2 elements when x=0.5. The dielectric constant and dielectric loss of polycrystalline samples of $La_{0.5}Li_{0.5-x}Na_xTiO_3$ have been investigated over a large frequency range. It has been found that the largest permittivity value is can be observed in $La_{0.5}Li_{0.4}Na_{0.1}TiO_3$ ceramic.



## 1. Introduction

Over the last years, solid lithium ion-conducting perovskites attract much interest [1–6] firstly reported by Belous et al. [7,8], due to their prospects for applications in gas sensors [9], cathodes in lithium batteries and as solid electrolytes [10]. Lanthanum lithium titanate is one of the highest lithium-ion conducting oxides, has been found to show lithium-ion conductivity as high as $10^{-3}$ S cm$^{-1}$ at room temperature [11]. La ions distribution affects the ionic conductivity. Conduction of Li ions occurs via vacancies in the A-site subcell of the perovskite $ABO_3$ structure [12] and is believed to be associated with lithium-ion transport through the so-called structural conduction channels i.e. "bottlenecks" formed by oxygen ions and A-site cations [13]. Larger channels provide lower activation energy of conductivity. La-site substitution in lanthanum lithium titanate with large cations (Na, K, Ag) or ions (Ba, Sr) has been reported to enlarge the "bottlenecks" dimensions, however, it leads to the deterioration of the lithium-ion conductivity due to the A-site vacancies concentration decrease [14–16]. Cation vacancies are disposed in alternating planes along the c-axis in Li-poor samples; whereas in Li-rich samples, vacancies become disordered [17]. In ceramic samples where lithium is partially replaced by sodium, Na ions occupy A sites of the perovskite while Li ions are located at the center of the square planar windows connecting contiguous A sites [7,8].

The contribution of mobile lithium ions to ion conductivity and low-frequency polarization depends on the number of structural vacancies in A-site and structural deformations [18]. It is important for the material design in high values of low-frequency dielectric constant.

Much attention is devoted nowadays to materials exhibiting the so-called giant dielectric constant for their potential technological applications [19–21]. In literature materials based on $BaTiO_3$ [22], NiO [23], CuO [24], ZnO [25] and $Bi_{0.5}Na_{0.5}TiO_3$ [26] exhibit giant dielectric permittivity phenomenon and have been widely investigated due to their potential applications in the microelectronic industry. High dielectric permittivity (ε≥1000) has been observed in polycrystalline samples of $La_{0.67}Li_{0.25}Ti_{0.75}Al_{0.25}O_3$, where titanium is partially substituted by aluminum. It has been demonstrated that the origin of the high dielectric constant can be attributed to a barrier layer capacitor associated with grain boundary effects in the ion-conducting material [27].

In this paper, the dielectric properties of partially Na-substituted $La_{0.5}Li_{0.5-x}Na_xTiO_3$ perovskite have been investigated. For this, impedance spectroscopy data of the $La_{0.5}Li_{0.5-x}Na_xTiO_3$ ($0 \le x \le 0.5$) series, recorded at room temperature, have been analyzed. Concerning cation mobility, impedance spectroscopy has been used to determine the equivalent circuit of lithium-conducting oxides. Scanning electron microscopy has been finally used to analyze the

* Corresponding author.
*E-mail address:* vyunov@ionc.kiev.ua (O.I. V'yunov).

https://doi.org/10.1016/j.jallcom.2021.161556
0925-8388/

influence of lithium concentration on the microstructure of these perovskites.

## 2. Experimental

Samples were obtained from stoichiometric amounts of dried $Li_2CO_3$ (Merck), $Na_2CO_3$ (Merck), $La_2O_3$ (Aldrich 99.99%) and $TiO_2$ (Aldrich 99%) by solid-state reaction technique. $Li_2CO_3$ and $Na_2CO_3$ compounds were dried at 300 °C, $La_2O_3$ at 800 °C and $TiO_2$ at 600 °C. The mixtures were ground in an agate mortar with acetone, and calcined in air for 4 h at 1100 °C. The rate of temperature increase was 200 °C/hour. The phases were characterized by X-ray powder diffractometry (XRPD) using DRON-4–07 diffractometer (Cu Kα radiation; 40 kV, 20 mA). The calcined powders were ground and pressed into pellets with a diameter of 16 mm and a thickness of 6 mm under a pressure of 500 kg/cm$^2$ (50 MPa). The pellets were sintered at 1300, 1306, 1312, 1318, 1324, 1330 °C depending on Na content (x=0, 0.1, 0.2, 0.3, 0.4, 0.5 respectively) for 6 h. Finally, samples with 1 mm thickness were cut out from prepared raw ceramic.

Grain sizes of ceramic samples of $La_{0.5}Li_{0.5-x}Na_xTiO_3$ system (where 0≤x≤0.5) were determined using a scanning electron microscope JEM 10CX II (JEOL) and scanning electron microscope SEC miniSEM SNE 4500MB equipped with EDAX Element PV6500/00 F spectrometer. Sintered cylindrical pellets 10 mm in diameter and 2 mm thick, with evaporated electrodes, were used for electrical measurements.

Impedance spectroscopy measurements were conducted using a 1260 Impedance/Gain phase Analyzer (Solartron Analytical). The equivalent circuit and the value of its components were determined using the ZView® software (Scribner Associates Inc., USA).

## 3. Results and discussion

XRD patterns of $La_{0.5}Li_{0.5-x}Na_xTiO_3$ samples at x=0–0.1 (Fig. 1) show the coexistence of rhombohedral symmetry (space group $R\bar{3}c$, No. 167) and tetragonal (space group P4/mmm, No. 123). At the same time, $La_{0.5}Li_{0.5-x}Na_xTiO_3$ solid solutions with x=0.2–0.5 are single-phase with a rhombohedral $R\bar{3}c$ symmetry. The observed rhombohedral and tetragonal phases do not differ in chemical composition. The main difference distinguishing these structures is that cation order occurs in the tetragonal unit cell, while the rhombohedral structure shows fully disordered A-site cations. Thus, sodium introduction leads to cation disordering [28,29]. Unit cell parameters

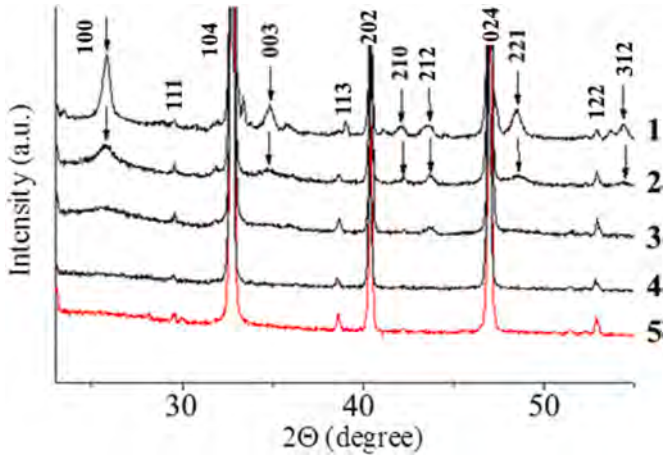


**Fig. 1.** XRPD of $La_{0.5}Li_{0.5-x}Na_xTiO_3$ of the rhombohedral phase at *x*=0 (1), 0.1 (2), 0.2 (3), 0.4 (4), 0.5 (5) (symbols "↓" denotes the additional phase with space group P4/mmm).

depend on sodium concentration, unit cell volume increases with an increase in x (Table 1).

The XRPD results showed that $La_{0.5}Li_{0.5-x}Na_xTiO_3$ (0≤x≤0.5) solid solutions are formed at temperatures higher than 1100 °C (Fig. 1). It has been shown that this is a multistage process.

In $La_{0.5}Li_{0.5-x}Na_xTiO_3$ sample (x=0) [30], the phase $La_{0.5}Li_{0.5}TiO_3$ appears as a result of partial interaction of the phases $Li_2Ti_2O_5$ and $La_2Ti_2O_7$ at temperature below 950 °C. An increase of temperature above 980 °C leads to the formation of the $La_{0.5}Li_{0.5}TiO_3$ phase (ICDD PDF-2 card #01-089-4928 [31]) as a result of interaction between $La_2O_3$ (#03-065-3185) and $Li_2Ti_3O_7$ (#00-040-0303 [32]). The final formation of the pure perovskite phase $La_{0.5}Li_{0.5}TiO_3$ takes place at a temperature above 1000 °C as a result of the reaction between $La_2Ti_2O_7$ (#01-070-0903) and $Li_2Ti_2O_5$ [33].

$$\frac{1}{4}La_2Ti_2O_7 + \frac{1}{4}Li_2Ti_2O_5 \xrightarrow{1000\,^{\circ}C} La_{0.5}Li_{0.5}TiO_3$$

Whereas a single-phase $La_{0.5}Li_{0.5-x}Na_xTiO_3$ solid solution (x=0.3) is formed at temperatures above 1080 °C [34]. Intermediate phases in Na-doped ceramics are $Na_4TiO_4$ (#01-080-1785), $Na_4Ti_5O_{12}$ (#01-075-2497), $Na_2Ti_2O_5$ (#mp-779477 [35]), $Li_2TiO_3$ (#01-071-2348), $Li_2Ti_2O_5$, $Li_2Ti_3O_7$, $La_2Ti_2O_7$, $La_{0.5}Li_{0.5}TiO_3$ and $La_{0.5}Na_{0.5}TiO_3$ (#01-089-4929). The $Na_2Ti_2O_5$ phase is formed through the intermediate $Na_4Ti_5O_{12}$ phase. And at the temperature higher 1000 °C it can be observed formation $La_{0.5}Na_{0.5}TiO_3$ and $La_{0.5}Li_{0.5}TiO_3$ phases, according to reactions:

$$\frac{x}{4}Na_2Ti_2O_5 + \frac{x}{4}La_2Ti_2O_7 \xrightarrow{1050\,^{\circ}C} xLa_{0.5}Na_{0.5}TiO_3$$

$$\frac{(1-x)}{4}La_2Ti_2O_7 + \frac{(1-x)}{4}Li_2Ti_2O_5 \xrightarrow{1000\,^{\circ}C} (1-x)La_{0.5}Li_{0.5}TiO_3$$

after all, solid solution $La_{0.5}Li_{0.5-x}Na_xTiO_3$ is formed by the interaction:

$$xLa_{0.5}Na_{0.5}TiO_3 + (1-x)La_{0.5}La_{0.5}TiO_3 \xrightarrow{1080\,^{\circ}C} La_{0.5}La_{0.5-x}Na_xTiO_3$$

Fig. 2 shows SEM photographs of $La_{0.5}Li_{0.5-x}Na_xTiO_3$ samples. The crystallite size of ceramics in $La_{0.5}Li_{0.5-x}Na_xTiO_3$ solid solutions decreases from 4.7 to 3 μm for x=0.1 and 0.4, respectively. This may be due to the partial segregation of $Na^+$ ions near the grain boundaries [36] and the reduction of their mobility on densification. This retards the mass transport and, as a result, smaller grains are formed [37]. Pores in the ceramics cause easy oxygen adsorption at the grain boundaries so that they are also more favorable to form surface acceptor states, compared with ordinary dense ones. It was previously shown [38] that an increase in sodium concentration leads to a decrease in the density of the sample, which may be due to the temperature difference between lithium and sodium carbonates. It is known that the melting point of lithium carbonate is lower than the melting point of sodium carbonate [39,40].

Fig. 3 shown the spectra imaginary part of complex electrical modulus of $La_{0.5}Li_{0.5-x}Na_xTiO_3$ ceramics at room temperature. The spectrum of Na-doped lithium-lanthanum titanate is of typical shape and includes three well-established dispersion regions [28]. Low-frequency region (marked as I-region) related to sample-electrode interface polarization, intermediate region (II-region) related to processes in grain boundaries and high-frequency region (III-region) related to charge carrier relaxation in grains. It can be assumed that the main contribution to electrical properties in the wide frequency range ($10^{-1}$≤*f*≤$10^7$ Hz) at room temperature of $La_{0.5}Li_{0.5-x}Na_xTiO_3$ (0≤x≤0.1) is made by II and III-regions, in $La_{0.5}Li_{0.5-x}Na_xTiO_3$ (0.2≤x≤0.4) is made by I, II, III-regions and in $La_{0.5}Li_{0.5-x}Na_xTiO_3$ (0.45≤x≤0.5) is made by I and III regions. This can be explained by the fact that the substitution of Li to Na leads to a decrease in the concentration of mobile charge carriers. Decrease of mobility occurs in grain boundaries of Na-doped lithium lanthanum

**Table 1**
Unit cell parameters of $La_{0.5}Li_{0.5-x}Na_xTiO_3$ samples with $R\bar{3}c$ space group.

| x | 0 | 0.1 | 0.2 | 0.3 | 0.4 | 0.5 |
|---|---|---|---|---|---|---|
| a, Å | 5.471(1) | 5.472(1) | 5.473(1) | 5.474(1) | 5.476(1) | 5.477(7) |
| c, Å | 13.402(4) | 13.404(3) | 13.402(3) | 13.405(4) | 13.406(4) | 13.417(2) |
| V, Å$^3$ | 347.4(2) | 347.6(2) | 347.7(2) | 347.9(2) | 348.1(2) | 348.6(9) |

titanate ceramics. Up to x≤0.3, the charge transport through the grains and grain boundaries take place, despite the reduced concentration of mobile Li ions due to blocking of conduction channels by Na. The M" maximum value of grain boundary (II-region, Fig. 3) with the increase in sodium concentration (0≤x≤0.4) increases that can be attributed to the limited mobility of lithium. In $La_{0.5}Na_{0.5}TiO_3$ there is no ion conductivity, the difference between grain bulk and grain boundary electrical properties is disappeared, and the material becomes dielectric.

Fig. 4a shows the complex impedance diagram at room temperature for $La_{0.5}Li_{0.4}Na_{0.1}TiO_3$ sample. One semicircle depressed below the real axis, part of a second semicircle and a spike at the lowest frequencies are observed. The arc at the highest frequencies is presented in the inset of Fig. 4a. For all samples $La_{0.5}Li_{0.5-x}Na_xTiO_3$ (0≤x≤0.5) the real part of the impedance increases with an increase in x (Fig. 4b).

The present experimental data (Fig. 4b) for $La_{0.5}Li_{0.5-x}Na_xTiO_3$ samples were analyzed according to the equivalent circuit represented earlier [28]. It has been found that the grain bulk and the grain boundary contribute to the electrical properties of the studied materials. Also, the sample-electrode area can be identified. Using the methodology of calculating the parameters of the equivalent circuit in [28] it has been shown these regions of the $La_{0.5}Li_{0.5-x}Na_xTiO_3$ ceramic are electrically inhomogeneous and characterize properties of grain bulk, grain boundary and electrode contact area. Resistances at the grain boundary (Rgb), grain volume (Rg) and at the electrode contact area (Rc) were given in Table 2.

According to our previous work [41], in $La_{0.5}Li_{0.5-x}Na_xTiO_3$ (0≤x≤0.5) Li ions occupy unit cell faces of the perovskite. From this fact, the amount of vacant A sites is higher than deduced from the structural formula. Based on structural and spectroscopic data, the number of vacant A-sites that participate in Li motion could correspond to the sum of nominal vacancies plus Li content. The conductivity of Li-rich samples (x < 0.2) is very high at room temperature, suggesting that A-sites associated with Li are not occupied and Li pass through square windows. In all perovskites the number of vacant sites is controlled by the amount of Na and La because Na and La ions are located at A sites, reducing the amount of vacant A sites that are pathways for ion motion. The amount of mobile Li ions decreases with the substitution of sodium for lithium in the $La_{0.5}Li_{0.5-x}Na_xTiO_3$ (0≤x≤0.5) series. When the sodium content increases above 0.2, conductivity is found to decrease.

It can be seen from Table 2, an increase in sodium concentration leads to an increase in Rg. Resistance in the bulk of the grains is determined by the concentration of free vacancies of Li and lithium concentration. In Na-doped ceramics, lithium-ion motion is limited

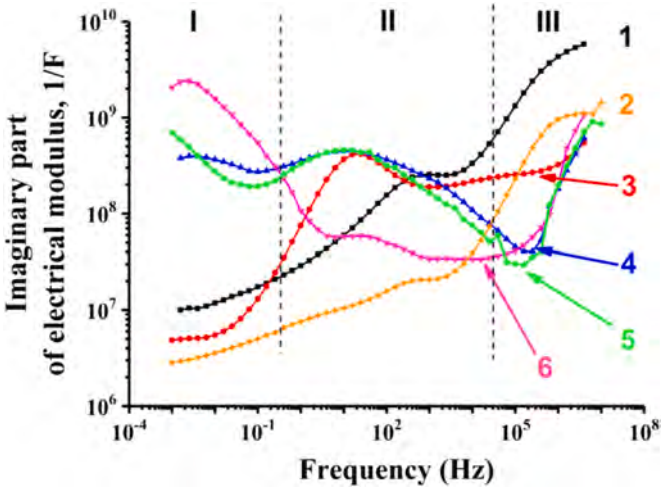


**Fig. 3.** Frequency dependences of imaginary part of electric modulus of $La_{0.5}Li_{0.5-x}Na_xTiO_3$ (b) at *x*=0 (1), 0.1 (2), 0.2 (3), 0.3 (4), 0.4 (5), 0.5 (6). Three observed dispersion regions are separated by vertical dotted lines and marked as I-region, II-region and III-region.

by fixed sodium ions in A-sites of the perovskite structure $ABO_3$. The increase in Rgb of the samples in $La_{0.5}Li_{0.5-x}Na_xTiO_3$ (0≤x≤0.5) is can be explained by the decrease in grain size (Fig. 2). With the decrease in grain size, the contribution of the grain boundary resistance in the total resistance increases.

Fig. 5 shows dielectric constant (Fig. 5a) and dielectric loss (Fig. 5b) versus frequency at room temperature. It has been shown that $La_{0.5}Li_{0.5-x}Na_xTiO_3$ samples (where x=0, 0.1) have high $\varepsilon' > 10^4$ at low frequencies ($f$≤10 Hz). It should be noted that with increasing sodium concentration, the maximum value of the dielectric constant decreases for samples where x is higher than 0.2.

Substitution of $Li^+$ ions by $Na^+$ ions in $La_{0.5}Li_{0.5-x}Na_xTiO_3$ solid solutions causes complex processes that affects the dielectric characteristics in the low-frequency and radio frequency ranges ($10^{-3}$–$10^6$ Hz). According to the Fig. 5 there are typically two frequency ranges of significant depression in ε accompanied by the tg δ maximum. We connect corresponding changes in ε and tg δ with a space-charge polarization for the frequency range of $10^{-3}$–$10^2$ Hz and an influence of $Li^+$ ionic conductivity, which has a noticeable effect in the frequency range of $10^2$–$10^6$ Hz.

The space-charge (migratory) polarization is a phenomenon observed in inhomogeneous dielectrics. Generally, it contributes to the dielectric constant in the low-frequency and radio frequency ranges

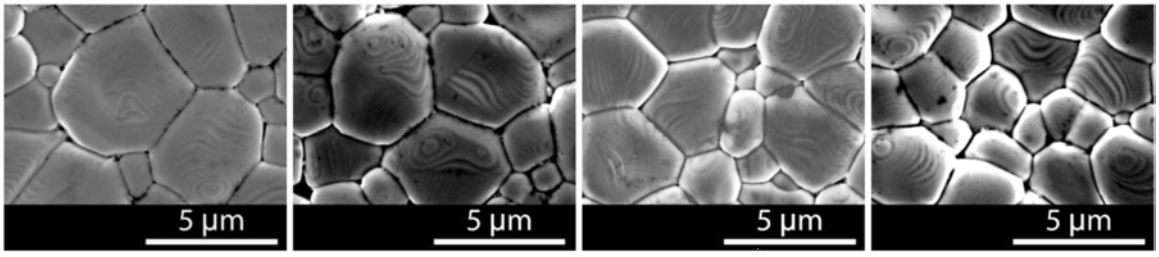


**Fig. 2.** Micrographs of $La_{0.5}Li_{0.5-x}Na_xTiO_3$ at *x*=0.1 (a), 0.2 (b), 0.3 (c), 0.4 (d).

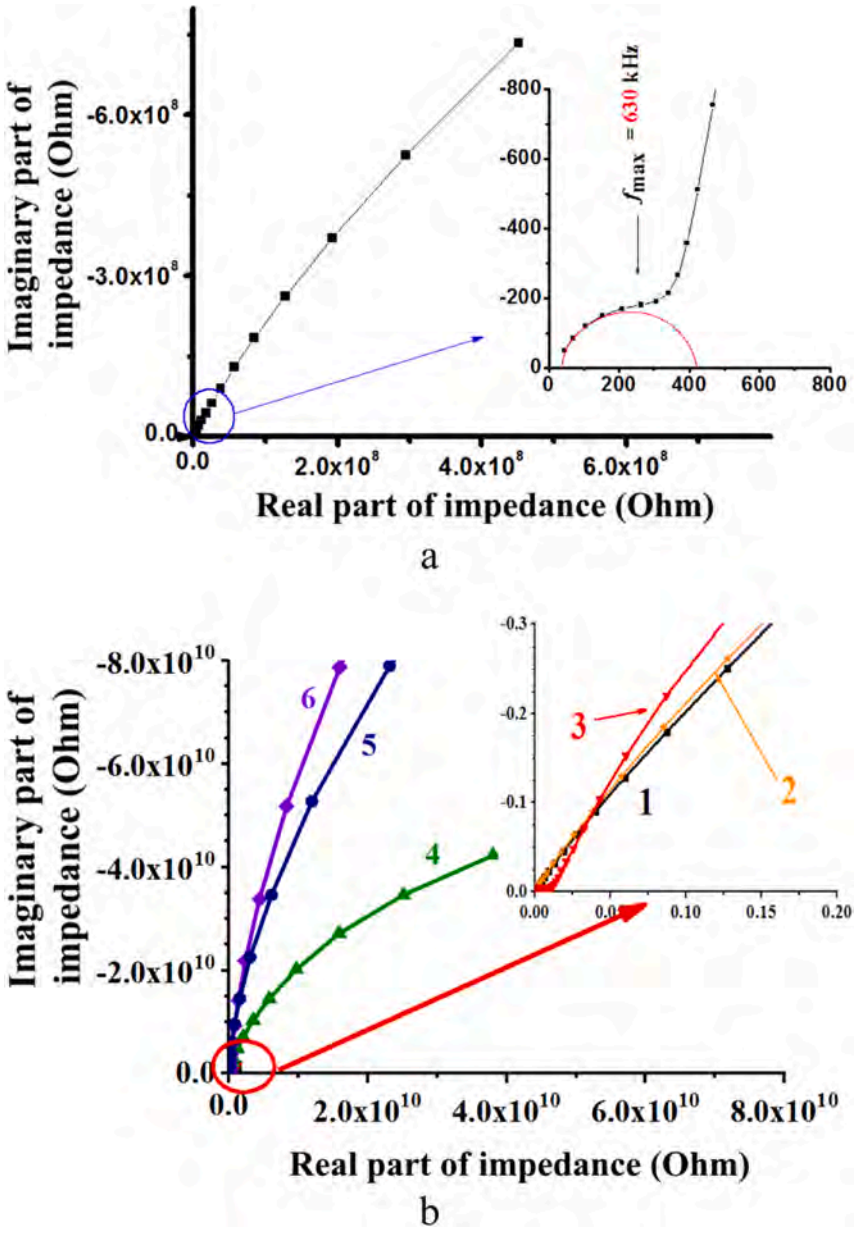


**Fig. 4.** Complex impedance diagram of $La_{0.5}Li_{0.4}Na_{0.1}TiO_3$ (a) and $La_{0.5}Li_{0.5-x}Na_xTiO_3$(b) at $x$=0 (1), 0.1 (2), 0.2 (3), 0.3 (4), 0.4 (5), 0.5 (6).

**Table 2**
Parameters of the equivalent circuits in polycrystalline $La_{0.5}Li_{0.5-x}Na_xTiO_3$ ($0 \le x \le 0.5$).

| [Na], x | Grain bulk Rg, Ohm | Grain boundary Rgb, Ohm | Contact area Rc, Ohm |
|---|---|---|---|
| 0 | 29.8 | $1.74 \cdot 10^3$ | $9.60 \cdot 10^8$ |
| 0.1 | 31.0 | $7.75 \cdot 10^3$ | $3.05 \cdot 10^9$ |
| 0.2 | 34.3 | $1.35 \cdot 10^7$ | $4.63 \cdot 10^9$ |
| 0.3 | 42.7 | $1.49 \cdot 10^7$ | $1.36 \cdot 10^{11}$ |
| 0.4 | 45.2 | $2.65 \cdot 10^7$ | $6.55 \cdot 10^{11}$ |
| 0.5 | $4.64 \cdot 10^7$ | | $9.77 \cdot 10^{11}$ |

($10^{-4}$–$10^4$ Hz) [42,43]. The accumulation of electric charges at the boundaries of inhomogeneities (and grain boundaries in particular) leads to space-charge polarization. The space charge significantly increases the dielectric capacity of the inhomogeneous capacitor. In the present work, the space-charge polarization makes a most significant contribution to the dependences $\varepsilon(f)$ and tg $\delta(f)$ in the frequency range of $10^{-3}$–$10^2$ Hz.

The dielectric constant is also affected by $Li^+$ ionic conductivity, the effect of which is noticeable in the frequency range of $10^2$–$10^6$ Hz. It is worth noting once again that the dependence of ionic conductivity on sodium content changes non-monotonic. With the increase in sodium content the unit cell volume increases (Table 1). On the one hand, the volume change leads to an increase in the $Li^+$ ions mobility and ionic conductivity increases. On the other hand, as the sodium content increases, the concentration of mobile $Li^+$ ions participating in ionic conductivity decreases. $Na^+$ ions are larger than $Li^+$ and don't move along conductive channels, formed by oxygen cuboctahedra. Therefore $Na^+$ ions do not participate in conductivity. At $x \ge 0.2$, the conductivity of the $La_{0.5}Li_{0.5-x}Na_xTiO_3$ system decreases with x.

A maximum bounded variance of $\varepsilon$ ($f$) in $La_{0.5}Li_{0.5}TiO_3$ is observed in the range of $10^4$–$10^6$ Hz. It is accompanied by a significant depression in $\varepsilon$ and the presence of a tg $\delta$ maximum (Fig. 5b curve 1). With the increase in $Li^+$ substitution on $Na^+$ ions in $La_{0.5}Li_{0.4}Na_{0.1}TiO_3$ the value of $Li^+$ ions mobility and also ionic conductivity ($\sigma_i$)

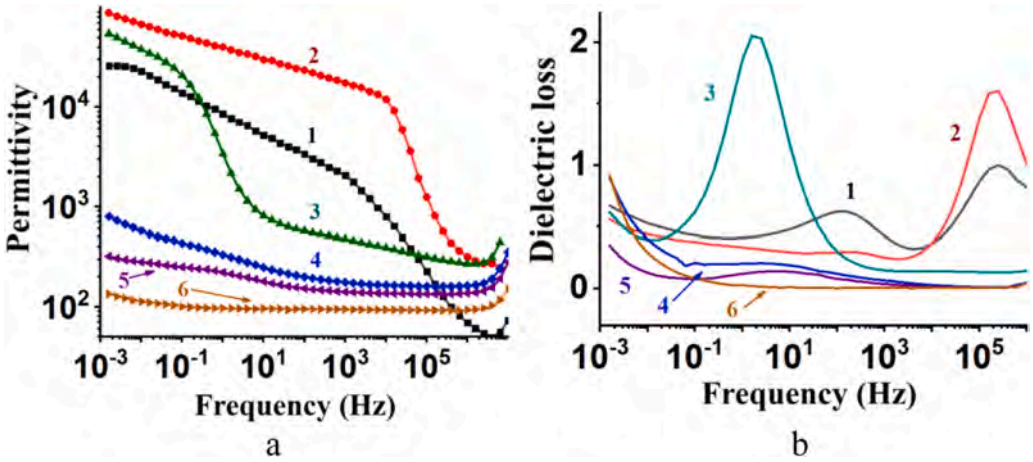


**Fig. 5.** Dielectric constant (a) and dielectric loss tangent (b) of $La_{0.5}Li_{0.5-x}Na_xTiO_3$ at $x$=0 (1), 0.1 (2), 0.2 (3), 0.3 (4), 0.4 (5), 0.5 (6).

**Table 3**
Dielectric constant and dielectric loss tangent in $La_{0.5}Li_{0.5-x}Na_xTiO_3$.

| x | ε′, 1 Hz | ε′, 10 Hz | ε′, $10^2$ Hz | ε′, $10^3$ Hz | ε′, $10^4$ Hz | tan δ (min) |
|---|---|---|---|---|---|---|
| 0 | 8600 | 5220 | 3370 | 2100 | 800 | 0.36 |
| 0.1 | 40100 | 30000 | 23500 | 17400 | 12000 | 0.25 |
| 0.2 | 3400 | 814 | 573 | 472 | 388 | 0.29 |
| 0.3 | 333 | 248 | 200 | 177 | 165 | 0.012 |
| 0.4 | 222 | 180 | 153 | 141 | 137 | 0.006 |
| 0.5 | 97 | 96 | 95 | 94 | 93 | 0.003 |

increases, which leads to an increase in ε. A decrease in ε (*f*), which is accompanied by a maximum on the tg δ (*f*) dependence, also occurs in the range of $10^4$–$10^6$ Hz in Fig. 5a, b, curve 2. Subsequent substitution of $Li^+$ ions by $Na^+$ ions ($La_{0.5}Li_{0.3}Na_{0.2}TiO_3$) leads to a decrease in ionic conductivity. As a consequence, a contribution to the value of ε from ionic conductivity decreases.

It can be seen from Table 3 that sample $La_{0.5}Li_{0.4}Na_{0.1}TiO_3$ has a maximum value of dielectric constant. This fact can be explained by two competing processes related to the movement of lithium ions. The dielectric response depends on the number of charge carriers that can shift and the distance by which they can shift. On the one hand, the increase in sodium substitution of lithium leads to an increase in unit cell volume (Table 1). The size of the so-called bottleneck, which limits the movement of lithium ions, also increases. As a result, an increase in sodium concentration can facilitate the migration of Li cations. On the other hand, lithium ions, which are located at the A-cage faces of the perovskite are substituted by sodium ions that are located in the centers of oxygen octahedrons. Thereby, vacancies that are conduction channels for lithium ions are filled by sodium ions. A rise in the degree of Li substitution leads to a decrease in lithium ions mobility. The amount of lithium ions also decreases when replaced by sodium ions. Thus, two different processes namely the increase in lithium ions mobility due to the growth of bottleneck size and the decrease due to a decrease in the number of vacancies leads to a maximum value of the dielectric constant in $La_{0.5}Li_{0.4}Na_{0.1}TiO_3$ ceramic sample.

## 4. Conclusions

Ceramic samples of $La_{0.5}Li_{0.5-x}Na_xTiO_3$ were synthesized by solid-state reaction technique. It has been shown that solid solutions are formed at temperatures higher than 1050 °C. Dielectric properties have been studied in ceramic $La_{0.5}Li_{0.5-x}Na_xTiO_3$ ($0 \le x \le 0.5$) by impedance spectroscopy. Using scanning electron microscopy, it has been found that the grain size of ceramics in $La_{0.5}Li_{0.5-x}Na_xTiO_3$solid solutions decreases from 4.7 to 3 μm for x=0.1 and 0.4, respectively. The dielectric loss increase with increasing in sodium concentration that can be attributed to the fact that the substitution of Li by Na decreases the lithium motion and reduces ion conductivity in the samples of $La_{0.5}Li_{0.5-x}Na_xTiO_3$ ($0 \le x \le 0.5$) system. The dielectric constant pass through a maximum ($\varepsilon \sim 4 \cdot 10^4$ at 1 Hz) in $La_{0.5}Li_{0.4}Na_{0.1}TiO_3$ ceramic. Two opposite processes can explain this maximum, namely the increase in lithium ions mobility due to the growth of bottleneck size and the decrease in lithium content and mobility due to a decrease in the number of vacancies.

## CRediT authorship contribution statement

**O.I. V'yunov:** Conceptualization, Investigation, Writing – original draft. **T.O. Plutenko:** Methodology, Resources, Writing – original draft. **O.P. Fedorchuk:** Investigation, Data curation. **A.G. Belous:** Supervision, Validation. **Ye.V. Lobko:** Research & Investigation, Analysis.

## Declaration of Competing Interest

The authors declare that they have no known competing financial interests or personal relationships that could have appeared to influence the work reported in this paper.

## Acknowledgements

The work was supported by the Research program of the Ukrainian National Academy of Sciences "New functional substances and materials for chemical production" (Fine Chemicals), project No. 0119U101351.

## Conflicts of interest

There are no conflicts to declare.

## References

[1] J.L. Ndeugueu, M. Aniya, On the power law behavior of the A.C. conductivity in Li ion conducting perovskites, J. Phys. Soc. Jpn. 79 (2010) 72–75, https://doi.org/10.1143/JPSJS.79SA.72
[2] C.H. Chen, S. Xie, E. Sperling, A.S. Yang, G. Henriksen, K. Amine, Stable lithium-ion conducting perovskite lithium–strontium–tantalum–zirconium–oxide system, Solid State Ion. 167 (2004) 263–272, https://doi.org/10.1016/j.ssi.2004.01.008
[3] X. Gao, C.A.J. Fisher, Y.H. Ikuhara, Y. Fujiwara, Sh Kobayashi, H. Moriwake, A. Kuwabara, K. Hoshikawa, K. Kohama, Cation ordering in A-site-deficient Li-ion conducting perovskites $La_{(1-x)/3}Li_xNbO_3$, J. Mater. Chem. A 3 (2015) 3351–3359, https://doi.org/10.1039/C4TA07040B

[4] W.J. Kwon, H. Kim, K. Jung, W. Cho, S.H. Kim, J. Lee, M. Park, Enhanced $Li^+$ conduction in perovskite $Li_{3x}La_{2/3-x}\square_{1/3-2x}TiO_3$ solid-electrolytes via microstructural engineering, J. Mater. Chem. A 5 (2017) 6257–6262, https://doi.org/10.1039/C7TA00196G

[5] Q.N. Pham, M.-P. Crosnier-Lopez, F. Le Berre, F. Fauth, J.-L. Fourquet, Crystal structure of new $Li^+$ ion conducting perovskites: $Li_{2x}Ca_{0.5-x}TaO_3$ and $Li_{0.2}[Ca_{1-y}Sr_y]_{0.4}TaO_3$, Solid State Sci. 6 (2004) 923–929, https://doi.org/10.1016/j.solidstatesciences.2004.05.006G

[6] J.-F. Wu, X. Guo, Origin of the low grain boundary conductivity in lithium ion conducting perovskites: $Li_{3x}La_{0.67-x}TiO_3$, Phys. Chem. Chem. Phys. 19 (2017) 5880–5887, https://doi.org/10.1039/c6cp07757a

[7] A.G. Belous, V.I. Butko, G.N. Novitskaya, Dielectric spectra of perovskites $La_{2/3-x}M_{3x}TiO_3$, Phys. Solid State 27 (1985) 2013–2016, https://doi.org/10.5281/zenodo.4146929

[8] A.G. Belous, V.I. Butko, G.N. Novitskaya, Electrical conductivity of perovskites $La_{2/3-x}M_{3x}TiO_3$, Ukr. J. Phys. 31 (1986) 576–581, https://doi.org/10.5281/zenodo.4091576

[9] S. Lorant, C. Bohnke, M. Roffat, O. Bohnke, New concept of an all-solid-state reference electrode using a film of lithium lanthanum titanium oxide (LLTO), Electrochim. Acta 80 (2012) 418–425, https://doi.org/10.1016/j.electacta.2012.07.051

[10] A. Belous, G. Kolbasov, L. Kovalenko, E. Boldyrev, S. Kobylianska, B. Liniova, All solid-state battery based on ceramic oxide electrolytes with perovskite and NASICON structure, J. Solid State Electrochem. 22 (2018) 2315–2320, https://doi.org/10.1007/s10008-018-3943-x

[11] Y. Inaguma, L. Chen, M. Itoh, T. Nakamura, T. Uchida, H. Ikuta, M. Wakihara, High ionic conductivity in lithium lanthanum titanate, Solid State Commun. 86 (1993) 689–693, https://doi.org/10.1016/0038-1098(93)90841-A

[12] Y. Inaguma, M. Itoh, Influences of carrier concentration and site percolation on lithium ion conductivity in perovskite-type oxides, Solid State Ion. 86–88 (1996) 257–260, https://doi.org/10.1016/0167-2738(96)00100-2

[13] A.G. Belous, Lithium ion conductors based on the perovskite $La_{2/3-x}Li_{3x}TiO_3$, J. Eur. Ceram. Soc. 21 (2001) 1797–1800, https://doi.org/10.1016/S0955-2219(01)00118-2

[14] H.-T. Chung, J.-G. Kim, H.-G. Kim, Dependence of the lithium ionic conductivity on the B-site ion substitution in $(Li_{0.5}La_{0.5})Ti_{1-x}M_xO_3$ (M=Sn, Zr, Mn, Ge), Solid State Ion. 107 (1998) 153–160, https://doi.org/10.1016/S0167-2738(97)00525-0

[15] O. Bohnke, C. Bohnke, J. Ould Sid'Ahmed, Lithium ion conductivity in new perovskite oxides $[Ag_yLi_{1-y}]_{3x}La_{2/3-x}\square_{1/3-2x}TiO_3$ ($x$=0.09 and 0≤y≤1), Chem. Mater. 13 (2001) 1593–1599, https://doi.org/10.1021/cm001207u

[16] A. Rivera, C. León, J. Santamaría, Percolation-limited ionic diffusion in $Li_{0.5-x}Na_xLa_{0.5}TiO_3$ perovskites (0≤x≤0.5), Chem. Mater. 14 (2002) 5148–5152, https://doi.org/10.1021/cm0204627

[17] J.A. Alonso, J. Sanz, J. Santamaría, C. León, A. Várez, M.T. Fernández-Díaz, On the location of $Li^+$ cations in the fast Li-cation conductor $La_{0.5}Li_{0.5}TiO_3$ perovskite, Angew. Chem. 39 (2000) 633–635, https://doi.org/10.1002/(SICI)1521-3773(20000204)39:3<619::AID-ANIE619>3.0.CO;2-O

[18] A.G. Belous, Temperature compensated microwave dielectrics based on lithium containing titanates, J. Eur. Ceram. Soc. 23 (2003) 2525–2528, https://doi.org/10.1016/S0955-2219(03)00185-7

[19] I.P. Raevski, S.A. Prosandeev, A.S. Bogatin, M.A. Malitskaya, L. Jastrabik, High dielectric permittivity in $AFe_{1/2}B_{1/2}O_3$ nonferroelectric perovskite ceramics (A=Ba, Sr, Ca; B=Nb, Ta, Sb), J. Appl. Phys. 93 (2003) 4130–4136, https://doi.org/10.1063/1.1558205

[20] Zh-M. Dang, B. Peng, D. Xie, Sh-H. Yao, M.-J. Jiang, J. Bai, High dielectric permittivity silver/polyimide composite films with excellent thermal stability, Appl. Phys. Lett. 92 (11) (2008) 112910, https://doi.org/10.1063/1.2894571

[21] F.B. Madsen, L. Yu, A.E. Daugaard, S. Hvilsted, A.L. Skov, Silicone elastomers with high dielectric permittivity and high dielectric breakdown strength based on dipolar copolymers, Polymer 24 (2014) 6212–6219, https://doi.org/10.1016/j.polymer.2014.09.056

[22] W. Jia, Y. Hou, M. Zheng, M. Zhu, High-temperature dielectrics based on (1-x)$(0.94Bi_{0.5}Na_{0.5}TiO_3$-$0.06BaTiO_3)$-x$NaNbO_3$ system, J. Alloys Compd. 724 (2017) 306–315, https://doi.org/10.1016/j.jallcom.2017.07.030

[23] J. Wu, C.-W. Nan, Y. Lin, Y. Deng, Giant dielectric permittivity observed in Li and Ti doped NiO, Phys. Rev. Lett. 89 (2002) 217601, https://doi.org/10.1103/PhysRevLett.89.217601

[24] Ch-L. Huang, K.-H. Chiang, Characterization and dielectric behavior of CuO-doped $ZnTa_2O_6$ ceramics at microwave frequency, Mater. Res. Bull. 39 (2004) 1701–1708, https://doi.org/10.1016/j.materresbull.2004.05.003

[25] G. Ioannou, A. Patsidis, G.C. Psarras, Dielectric and functional properties of polymer matrix/ZnO/$BaTiO_3$ hybrid composites, Compos. Part A 42 (2011) 104–110, https://doi.org/10.1016/j.compositesa.2010.10.010

[26] F. Han, J. Deng, X. Liu, T. Yan, Sh Ren, X. Ma, S. Liu, B. Peng, L. Liu, High-temperature dielectric and relaxation behavior of Yb-doped $Bi_{0.5}Na_{0.5}TiO_3$ ceramics, Ceram. Int. 43 (2017) 5564–5573, https://doi.org/10.1016/j.ceramint.2017.01.086

[27] S. García-Martín, A. Morata-Orrantia, M.H. Aguirre, M.Á. Alario-Franco, Giant barrier layer capacitance effects in the lithium ion conducting material $La_{0.67}Li_{0.25}Ti_{0.75}Al_{0.25}O_3$, Appl. Phys. Lett. 86 (4) (2005) 043110, https://doi.org/10.1063/1.1852717

[28] E. Kazakevičius, A. Kežionis, T. Šalkus, A.F. Orliukas, O.I. V'yunov, L.L. Kovalenko, A.G. Belous, Some aspects of charge transport in $Li_{0.5-x}Na_xLa_{0.5}TiO_3$ (x=0, 0.25) ceramics, Funct. Mater. Lett. 08 (2015) 1550076, https://doi.org/10.1142/S1793604715500769

[29] M.L. Sanjuan, M.A. Laguna, A.G. Belous, O.I. V'yunov, On the local structure and lithium dynamics of $La_{0.5}(Li,Na)_{0.5}TiO_3$ ionic conductors. A Raman study, Chem. Mater. 23 (2005) 5862–5866, https://doi.org/10.1021/cm0517770

[30] A.D. Robertson, S. Garcia Martin, A. Coats, A.R. West, Phase diagrams and crystal chemistry in the Li+ ion conducting perovskites, $Li_{0.5-3x}RE_{0.5+x}TiO_3$: RE=La, Nd, J. Mater. Chem. 5 (1995) 1405–1412, https://doi.org/10.1039/JM9950501405

[31] S. Gates-Rector, T. Blanton, The powder diffraction file: a quality materials characterization database, Powder Diffr. 34 (2019) 352–360.

[32] H. Izawa, S. Kikkawa, M. Koizumi, K. Yogyo, Properties of layered titanate, $H_2Ti_3O_7$, as an inorganic ion-exchanger for lithium, J. Ceram. Assoc., Jpn. 94 (1986) 621–624, https://doi.org/10.2109/jcersj1950.94.1091_621

[33] A. Miller, R. Carchman, R. Long, S.A. Denslow, La Crosse viral infection in hospitalized pediatric patients in Western North Carolina, Nat. Library Med. 2 (4) (2012) 235–242, https://doi.org/10.1542/hpeds.2012-0022

[34] T.O. Plutenko, O.I. V'yunov, O.P. Fedorchuk, O.Z. Yanchevskii, A.G. Belous, Formation during the synthesis and dielectric properties of $La_{0.5}Li_{0.5-x}Na_xTiO_3$, Ukr. Chem. J. 87 (2021) 3–12, https://doi.org/10.33609/2708-129X.87.05.2021.3-12

[35] K. Persson, Materials Data on Na2Ti2O5(SG:14) by Materials Project, in, United States, 2016. doi: 10.17188/1306406.

[36] S.B. Desu, D.A. Payne, Interfacial segregation in perovskites: II, experimental evidence, J. Am. Ceram. Soc. 73 (1990) 3398–3406, https://doi.org/10.1111/j.1151-2916.1990.tb06467.x

[37] C. Zhou, X. Liu, W. Li, C. Yuan, Structure and piezoelectric properties of $Bi_{0.5}Na_{0.5}TiO_3$–$Bi_{0.5}K_{0.5}TiO_3$–$BiFeO_3$ lead-free piezoelectric ceramics, Mater. Chem. Phys. 114 (2009) 832–836, https://doi.org/10.1016/j.matchemphys.2008.10.063

[38] A.G. Belous, Properties of lithium ion-conducting ceramics based on rare-earth titanates, Ionics 4 (1998) 360–363, https://doi.org/10.1007/BF02375878

[39] D.R. Lide, Lithium carbonate, Handbook of Chemistry and Physics 86TH Edition, CRC Press, Taylor & Francis, Boca Raton, FL, 2005-06, pp. 4–70.

[40] A.E. Newkirk, I. Aliferis, Drying and decomposition of sodium carbonate, Anal. Chem. 30 (1958) 982–984, https://doi.org/10.1021/ac60137a031

[41] C.P. Herrero, A. Varez, A. Rivera, J. Santamarıa, C. Leon, O. V'yunov, A.G. Belous, J. Sanz, Influence of vacancy ordering on the percolative behavior of $(Li_{1-x}Na_x)_{3y}La_{2/3-y}TiO_3$ perovskites, J. Phys. Chem. B 109 (2005) 3262–3268, https://doi.org/10.1021/jp046076p

[42] Y.M. Poplavko, Dielectrics, Electronic Materials, Elsevier, 2019, pp. 287–408, https://doi.org/10.1016/b978-0-12-815780-0.00007-4

[43] R. Gu, K. Yu, L. Wu, R. Ma, H. Sun, L. Jin, Y. Xu, Z. Xu, X. Wei, Dielectric properties and I–V characteristics of $Li_{0.5}La_{0.5}TiO_3$ solid electrolyte for ceramic supercapacitors, Ceram. Int. 45 (2019) 8243–8247, https://doi.org/10.1016/j.ceramint.2019.01.128